FUNGAL BIOLOGY 115 (2011) 493–505

British Mycological Society promoting fungal science

journal homepage: www.elsevier.com/locate/funbio

Probing the growth dynamics of *Neurospora crassa* with microfluidic structures

Marie HELD[a], *Clive EDWARDS*[b], *Dan V. NICOLAU*[a,*]

[a]*Department of Electrical Engineering & Electronics, University of Liverpool, Liverpool L69 3GJ, United Kingdom*
[b]*School of Biological Sciences, University of Liverpool, Liverpool L69 7ZB, United Kingdom*

ARTICLE INFO

Article history:
Received 10 November 2010
Received in revised form
26 January 2011
Accepted 2 February 2011
Available online 24 February 2011
Corresponding Editor:
Brian Douglas Shaw

Keywords:
Apical extension
Fungal branching
Fungal growth
Microfluidics
Neurospora crassa
PDMS
ro-1 mutant

ABSTRACT

Despite occupying physically and chemically heterogeneous natural environments, the growth dynamics of filamentous fungi is typically studied on the surface of homogeneous laboratory media. Fungal exploration and exploitation of complex natural environments requires optimal survival and growth strategies at the colony, hyphal, and intra hyphal level, with hyphal space-searching strategies playing a central role. We describe a new methodology for the characterisation and analysis of hyphal space-searching strategies, which uses purposefully designed three-dimensional microfluidics structures mimicking some of the characteristics of natural environments of the fungi. We also demonstrate this new methodology by running a comparative examination of two *Neurospora crassa* strains, i.e., the wild type of *N. crassa* – a commonly used model organism for the study of filamentous fungi – and the *N. crassa ro-1* mutant strain – which is deficient in hyphal and mycelial growth. Continuous live imaging showed that both strains responded actively to the geometrically confined microstructured environments without any detectable temporal delay or spatial adjustment. While both strains navigated the test structures exhibiting similar geometry-induced space-searching mechanisms, they presented fundamentally different growth patterns that could not be observed on geometrically unconfined, flat agar surfaces.

Introduction

Filamentous fungi form a group of microorganisms that have a significant ecological and economical impact as decomposers of biomass and as pathogens of plants, animals, and humans (Evans & Hedger 2001). The habitats colonised by fungi comprise a wide range of microstructured environments that are also chemically and physically heterogeneous. The exploration and exploitation of these environments requires the fungus to respond efficiently to stimuli that are spatially distributed at the macro and microscale, as well as variable in time. In order to conduct these phenotypic responses, both at the colony and individual hypha level, filamentous fungi have developed efficient strategies to optimise their growth. While at the macro-, colony-scale, filamentous fungi can relocate large fractions of mycelial matter (Fricker *et al.* 2008), at the level of individual hyphae, fungal growth dynamics is driven by a variety of sensing mechanisms manifested at the extending apex (Kumamoto 2008). This specific location provides a means to gain dynamic information about the physical (e.g., available space, distribution of light) and chemical (e.g., distribution of nutrients, toxins) properties of the environment. Despite this microscale dependent behaviour, fungal growth has been studied primarily in and on homogeneous media (Fricker *et al.* 2008; Kasuga & Glass 2008; Gougouli & Koutsoumanis 2010) that bear little or no resemblance to

* *Corresponding author*. Tel.: +44 151 794 4537; fax: +44 151 794 4540.
E-mail address: dnicolau@liverpool.ac.uk
1878-6146/$ – see front matter
doi:10.1016/j.funbio.2011.02.003

their natural habitats. The experimental and computational studies that were conducted on heterogeneous media by Boddy *et al*. investigated the mycelial foraging and relocation of biomass upon a temporal change in the environment (Boddy 1999; Boswell *et al*. 2007; Fricker *et al*. 2008; Boddy *et al*. 2009). These studies observed and simulated the large-scale spatial and temporal development of the whole mycelium on a centimetre scale but not the individual hyphae or their apical compartments in particular.

Taking advantage of the well-established fabrication methods of semiconductor technology (Duffy *et al*. 1998; Menz *et al*. 2001), artificial structures in the micrometre range resembling the spatial properties of the habitat of filamentous fungi can be routinely fabricated. For instance, pores with diameters in the low micrometre range, filled with a nutrient medium, resemble the body of plant cells within the cell walls; complex and/or periodic channel networks mimic the apoplast in between the primary cell walls of plants whereas thin membranes mimic a resistance that needs to be overcome by appressoria (Bechinger *et al*. 1999; Apoga *et al*. 2004). Aside of the geometrical resemblance to the natural microenvironment, the microstructures probing the fungal behaviour should be fabricated from a material that also has a reasonable level of similarity with respect to its mechanical and physiochemical characteristics. Fortunately, one of the most popular materials used for the mass fabrication of artificial microconfined structures, the silicon-based polymer Poly(DiMethylSiloxane) (PDMS), provides this opportunity. Compared with conventional microfabrication materials, such as silicon and glass, which are expensive to process and only present a limited biocompatibility, microfluidic devices made of polymers in general, and PDMS in particular, are cheaper, their fabrication is simpler and does not require clean room facilities. PDMS fabrication *via* soft lithography commonly involves rapid replica moulding from a negative relief master made of silicon (Duffy *et al*. 1998; McDonald *et al*. 2000), or a hard negative tone photoresist like SU-8 (Ghantasala *et al*. 1999; Ghantasala *et al*. 2001) or Hydrogen SilsesQuioxane (HSQ) (van Delft *et al*. 2010). Additionally, cured PDMS has the advantage of being transparent down to 280 nm, thus allowing a variety of detection methods at a wide range of wavelengths (Lötters *et al*. 1997; Duffy *et al*. 1998; McDonald *et al*. 2000; Merkel *et al*. 2000; Lee *et al*. 2003; Sia & Whitesides 2003). The cured polymer is biologically and chemically inert, non-toxic and oxygen and carbon dioxide permeable. Furthermore, it seals readily and reversibly with other silicon-based materials and its surface chemistry can be modified easily. Due to its biocompatibility, PDMS has been used extensively in biological research projects. These include sensor (Park & Shuler 2003) and tissue engineering (Folch & Toner 1998; Desai 2000; Jiang *et al*. 2005), manipulation of cell shape (Singhvi *et al*. 1994a, 1994b; Chen *et al*. 1998; Kane *et al*. 1999; Leclerc *et al*. 2003), function and migration (Jiang *et al*. 2005; Hanson *et al*. 2006), examination of individual cell and population-level bacterial behaviour (Binz *et al*. 2010; Park *et al*. 2003a, 2003b), diagnostic cell arrays (Ziauddin & Sabatini 2001; Griscom *et al*. 2002), and biocomputation (Hanson *et al*. 2006).

The growth of filamentous fungi is uniquely characterised by the formation of radially expanding, circular colonies. The mechanisms underlying this growth pattern are the highly polarised hyphal extension at the apex (Molin *et al*. 1992; Riquelme *et al*. 1998; Momany 2002; Harris & Momany 2004), periodic hyphal branching (Katz *et al*. 1972; Watters *et al*. 2000a, 2000b; Riquelme & Bartnicki-Garcia 2004), and negative autotropism (Trinci 1974; Robinson & Bolton 1984). Despite increasing efforts to identify the specific biological mechanisms and organelles responsible for the polarisation of hyphal growth and the regular branching pattern, these mechanisms still require considerable examination. The efforts to investigate the biological fundamentals of hyphal growth include light microscopy (Brunswick 1924; Girbardt 1969; Freitag *et al*. 2004; Fricker *et al*. 2008; Uchida *et al*. 2008), electron microscopy (Girbardt 1969; Grove & Bracker 1970; Riquelme *et al*. 2002), chemical (Riquelme *et al*. 1998), genetic (Emerson 1963; Riquelme *et al*. 2002; Seiler & Plamann 2003; Verdín *et al*. 2009), and theoretical (Bartnicki-Garcia *et al*. 1989; Riquelme *et al*. 1998; Klumpp & Lipowsky 2003; Darrah *et al*. 2006; Hanson *et al*. 2006; Nicolau *et al*. 2006; Sugden *et al*. 2007) approaches.

To this end, we propose a new experimental methodology based on the observation of fungal growth in artificial structures mimicking some of the characteristics of their natural environment. Several groups have investigated the influence of microscale topographies on fungal growth and found that filamentous fungi exhibit thigmotropism, i.e., direct hyphal growth in response to contact stimuli (Hoch *et al*. 1987; Brand *et al*. 2008; Held *et al*. 2009c). We have previously shown that growth of filamentous fungi in microfluidic channel networks triggers a significantly altered behaviour compared with that in open flat environments, leading to a considerable morphological alteration (Hanson *et al*. 2006; Held *et al*. 2008; Held *et al*. 2009a, 2009b; Held *et al*. 2010). These studies suggest that purposefully designed microfluidic structures can provide a new methodology to study the biological fundamentals promoting fungal growth in general and apical extension in particular. The present study compares the growth dynamics of the *Neurospora crassa* wild type and a *N. crassa ro-1* mutant (lacking the heavy chain of dynein) on agar and within microfluidic test structures. *Neurospora crassa* was chosen for this study because it has been the subject of extensive research over several decades (Ryan *et al*. 1943; Trinci & Collinge 1973; Vaughn & Davis 1981; Riquelme *et al*. 1998; Watters *et al*. 2000a; Momany *et al*. 2002; Silverman-Gavrila & Lew 2003; Riquelme & Bartnicki-Garcia 2004; Wright *et al*. 2007; Kasuga & Glass 2008) and a variety of mutants is readily available (Beadle & Tatum 1945; Emerson 1963; Riquelme *et al*. 2002; Seiler & Plamann 2003). The *N. crassa* wild type exhibits the characteristic growth patterns of filamentous fungi. The *ro-1* mutant is viable and able to develop large colony radii. It exhibits a fundamentally different growth pattern characterised by the lack of maintenance of growth in fixed directions and significantly increased branching. Therefore, this mutant strain provided a significant counterpoint to the behaviour of the wild type.

Materials and methods

Growth and maintenance of cultures

The *Neurospora crassa* wild type strain used in this study was obtained from the culture collection of the School of Biological

Sciences (University of Liverpool, Liverpool, UK). The *N. crassa ro-1* mutant strain (FGSC #110) was obtained from the Fungal Genetics Stock Center (School of Biological Sciences, University of Missouri, Kansas City, MO, USA). The *ro-1* mutant strain exhibits a highly irregular hyphal morphology resulting in hyphae that are curled, have reduced apical extension rates and altered Spitzenkörper organisation and behaviour (Garnjobst & Tatum 1967). Both strains were maintained on 1 % malt extract agar (Merck) at 4 °C. Prior to each experiment, the fungal strains were sub-cultured onto malt extract agar plates and incubated at room temperature for 24 h.

Microfabrication

The microfluidic networks, designed to allow only two hyphae per channel, were fabricated using the transparent, biocompatible polymer PDMS (Sylgard 184, Dow Corning) following the flow chart represented in Fig 1A. A positive relief silicon master (provided by Prof. Lee, University of California, Irvine, CA, USA) was fabricated using standard photolithography techniques and subsequent deep reactive ion etching (Hanson *et al.* 2006). HexaMethylDiSilazane (HMDS) was evaporated on this positive relief master to render its surface hydrophobic, then the negative relief PDMS stamp was fabricated by casting a mixture of degassed PDMS pre-polymer and its curing agent (10:1 by weight) according to well-established protocols (Sia & Whitesides 2003). The PDMS was cured at 65 °C for at least 8 h to ensure full cross-linking of the polymer. After removal from the silicon master both the PDMS surface and the surface of a flat glass base layer (microscope slide) were rendered hydrophilic by deep UV/ozone exposure using a UVO cleaner. The exposure caused the formation of silanol groups on both surfaces. Bringing these surfaces into contact resulted in the formation of covalent bonds under water condensation so that the microfluidic structures were sealed irreversibly to the microscope slide. We used three different types of microfluidic structures, all with a channel depth of 10 μm. The largest channels had a constant width of 1000 μm and the medium channels had a constant width of 100 μm. The smallest and most complex microfluidic test structures (Fig 1B and C) had a total edge length of 100 μm. The channel and feature sizes within the networks had dimensions similar to the hyphal diameter (average: 7 μm). The 'small maze' structure consisted of a variety of features with sizes ranging from 5 μm to 25 μm, comprising diverse, complex, and non-periodic shapes. In contrast, the diamond structure consisted of a square pattern of 16 10 μm × 10 μm wide pillars positioned at regular intervals. The entrance and exit were positioned at two opposite corners, which resulted in two different kinds of solution paths, including a periodic path through the pillars and a rather straight path around the pillar pattern.

Experimental setup

The microfluidic networks were designed to present lateral openings for the introduction of growth medium and fungal hyphae into the enclosed areas. The microstructures were filled with sterile distilled water by immersion of the structure and subsequent evacuation of the setup in a desiccator.

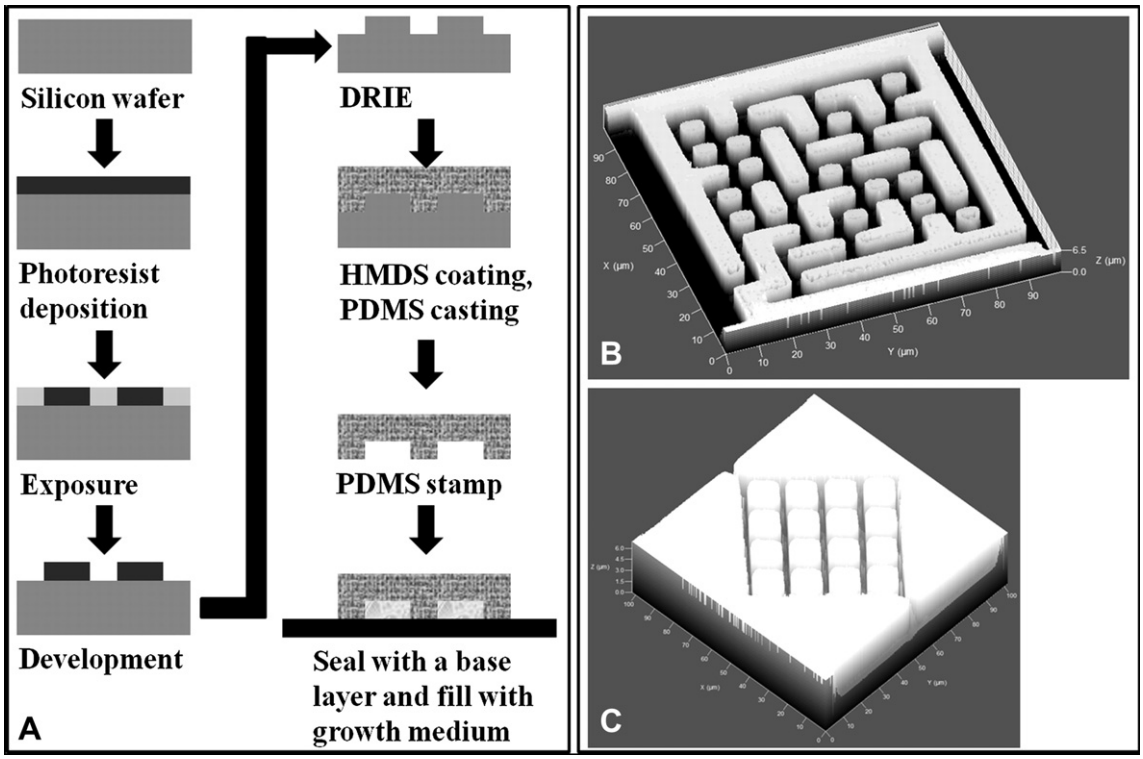

Fig 1 – (A) Flow chart of the fabrication process of microstructured Si wafers and subsequent PDMS moulds. (B) A three-dimensional representation of the 'small maze' structure and (C) A three-dimensional representation of the 'diamond' structure used.

Fungal inoculation was achieved by placing an agar plug from the peripheral growth zone of a colony next to the lateral opening of the PDMS structure. This assembly was then enclosed in a Petri dish to retain the moisture but also to allow the exchange of oxygen and carbon dioxide.

Imaging and data analysis

Live cell imaging of hyphal growth on agar and inside the microfluidic structures was performed on a Brunel inverted microscope (SPI-98) equipped with a digital camera (Moticam 2300 3 MP) and with an inverted Zeiss Axio Observer Z1 equipped with a photomultiplier. The images were typically recorded as time series at regular intervals (usually one frame per 15–30 s). For frame-by-frame tracking and calculation of the hyphal kinetics, RETRAC 2.10.0.5 (shareware by Nick Carter) was employed and Statistica 7.1 (Statsoft Inc., OK, USA) was used for statistical analysis. The statistical analysis of the images comprised the measuring of the apical extension velocity, branching angle (angle between the parent and the daughter hypha at the branching point), and the branching distance (distance between two subsequent branching points along a parent hypha). The measurement of these parameters was performed on growing hyphae in the colony margin, excluding leading hyphae. The statistical analysis included the mean and standard deviation values of these parameters.

Biomass distributions were determined as the occupancy of the channels by *Neurospora crassa* hyphae averaged over a number of different experiments i. In order to systematise this parameter, the 100 μm × 100 μm structures (edge length) were divided into a raster of 'pixels' width dimensions of 5 μm × 5 μm (with n the total number of pixels that represent channels, i.e., that can be occupied by fungal hyphae). For each structure and strain we counted how often a pixel had been occupied, summed up over the total number of experiments (p_i). These counts were then normalised with the maximum count (p_{max}) in each respective microfluidic structure and the total counts per pixel were replaced with a scale factor (sf_i) determined as $sf_i = p_i/p_{max}$ that ranges from 0 to 1. The scale factor can be used as a measure of the average occupancy of the fungal strains in the microfluidic structures. In order to do that, the average scale factor $\overline{sf}$ of each structure was calculated as $\overline{sf} = \sum_{i=1}^{n} sf_i/n$.

Results and discussion

Growth dynamics on agar plates

The growth dynamics of both *Neurospora crassa* strains grown on malt extract agar plates differed significantly from each other. The two strains also exhibited a considerable modification in the morphology of the individual hyphae and the colonies as a whole. Generally, the *N. crassa* wild type exhibited the typical growth observed in most filamentous fungi, whereas the *ro-1* mutant exhibited curled hyphae and a higher hyphal density within the colony (Fig 2A and B).

Measurable growth parameters

The growth dynamics of the *Neurospora crassa* wild type was characterised by the typical apical extension of filamentous fungi with an average apical extension velocity of 12.5 μm min^{-1} (Table 1). This apical extension velocity was measured for growing hyphae that were not leading hyphae. The probability of a leading hypha entering the microfluidic channels was negligible and therefore their contribution to the average growth parameters on agar was excluded from the statistical analysis. The general apical extension velocity averaged overall cell types combined with a fixed growth direction of individual hyphae resulted in a colony extension of 4–5 cm over 24 hours. Branching was exclusively lateral and occurred regularly at an average interval of 219 μm and with a mean branching angle of 45° between the parent and the daughter hyphae (Fig 2C). These growth parameters of the wild type, which lie within the ranges given in the literature, resulted in an efficient exploration (homogeneous distribution of hyphae) and therefore exploitation of the homogeneous agar surface. While the apical extension velocity of the *ro-1* mutant was only slightly lower (8.1 μm min^{-1}) compared with that of the wild type strain, the curled hyphal morphology resulted in a considerably reduced colony extension. This divergence in behaviour also manifested in the branching angle that was approximately double than that of the wild type (94.4°) – combined with a partially dichotomously branching pattern – and a branching distance that was reduced by a factor of 6.5 to 34.3 μm. Of these three parameters, the mutation of the *ro-1* strain appeared to mainly affect the branching distance. Overall, the combination of these parameters resulted in a moderate rate of colony extension of

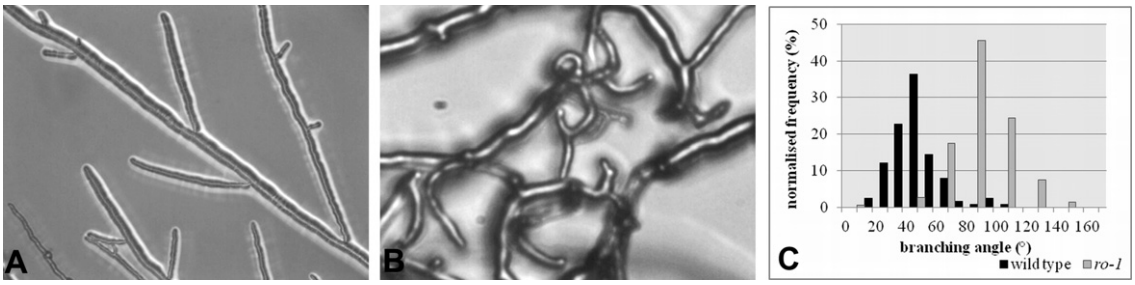

Fig 2 – Overview of the fungal growth patterns observed on the surface of malt extract agar. Images A and B show light microscopy images growth of the *Neurospora crassa* wild type (A) and *ro-1* mutant (B) respectively. The wild type exhibits the typical fungal growth with polarised extension and periodic branching whereas the *ro-1* mutant exhibits curled hyphae. Image (C) represents the distributions of the branching angles measured for *N. crassa* wild type and *ro-1* on the agar surface.

Table 1 – Overview of the growth parameters of the *N. crassa* wild type and *ro-1* mutant strain on agar and within two microfluidics test structures. The exit *versus* entrance rate is the ratio of the number of hyphae exiting the structures *versus* the total number of hyphae that entered the structure initially. For the diamond structure the values are larger than one because of the branching of hyphae inside the structure, which enabled several hyphae to find the exit from the same structure. The brackets enclose the numbers of data points for every parameter.

Parameter	*N. crassa* wild type			*N. crassa ro-1*		
	Agar	Diamond	Small maze	Agar	Diamond	Small maze
Branching angle (°)	45.0 ± 16.0 (125)	91.2 ± 5.4 (63)	93.3 ± 15.4 (84)	94.4 ± 19.4 (329)	88.8 ± 12.9 (45)	89.4 ± 9.0 (53)
Branching distance (μm)	219.1 ± 126.4 (107)	43.1 ± 40.1 (67)	23.5 ± 15.0 (77)	34.3 ± 26.2 (221)	50.8 ± 38.4 (46)	17.7 ± 9.0 (51)
Apical extension velocity (μm/min)	12.5 ± 10.2 (1884)	1.8 ± 0.9 (2350)	0.8 ± 0.5 (2215)	8.1 ± 3.8 (2751)	2.1 ± 1.2 (1185)	1.2 ± 0.7 (2308)
Exit *versus* entrance rate	–	1.23 (185)	0.90 (80)	–	1.35 (20)	0.73 (11)
Average scale factor	–	0.32 (65)	0.42 (169)	–	0.36 (65)	0.49 (169)

approximately 1.5 cm over 24 h and a significantly higher hyphal density of the colony of the *ro-1* mutant compared with that of the wild type strain.

Polarity of growth

The hyphae of the *Neurospora crassa* wild type maintained fixed growth directions with the polarisation axes determined at the respective branching points (Fig 2A). Even though the strain was not spatially confined in this setup, it exhibited a non-uniform distribution along the vertical axis in the agar, i.e., it appeared to be drawn to the surface of the agar medium. The growth dynamics of the *N. crassa ro-1* mutant was dominated by a steady apical extension, although the lack of maintenance of the polarisation axis of individual hyphae ultimately resulted in curled hyphae (Fig 2B). In contrast to the wild type, the *ro-1* mutant seemed less attracted to the surface of the agar medium.

Growth dynamics in 1000 μm channels

In contrast to agar substrates, the 1000 μm wide channels confined the fungi in the vertical dimension. As well as the spatial limitation, the experimental setup circumvented a non-uniform distribution of oxygen and nutrients in the z-direction. Time-lapse imaging of both *Neurospora crassa* strains grown in 1000 μm wide and 10 μm deep channels showed that the hyphae responded strongly to the geometrical properties of their environment. Overall, the alterations of the growth dynamics promoted the continued extension of hyphae through the confined areas and away from the colony centre. The wild type maintained its lateral, periodic branching pattern albeit with a reduced average branching distance of 163 μm and an increased average branching angle of 65.4°. When a hypha of the wild type grew in close contact with a wall, it usually branched on the hyphal side facing away from the wall, thus resulting in the branches growing away from the obstacle (Fig 3A). In case of the *ro-1* mutant, the partially dichotomous branching pattern observed on agar became exclusively lateral (Fig 3B) in the 1000 μm wide channels. When a hypha grew along or in close proximity to a wall, branches were formed predominantly towards the wall, a behaviour opposite to the one observed for the wild type. This branching pattern usually resulted in the growing daughter hyphae pushing the parent hypha away from the wall, into the open channel. The wild type branching pattern away from the wall could result in the biological benefit of directing the growth away from the obstacle and thus an increased probability of finding new nutrient sources. On the other hand, the 'handedness' of the branching of the mutant strain towards the wall had no apparent biological benefit. These observations suggest that the trigger for the space-searching mechanism directing the branches away from the wall was affected by the mutation. Furthermore, they support the hypothesis that the mutation has the most impact on branching in general. In contrast to the wild type, it appeared that the *ro-1* mutant exhibited a particular affinity to the confining walls of the 1000 μm wide channels. Once established, the hyphae maintained wall contact for long periods, thus preventing it from exploring the bulk of the 1000 μm wide channel. This altered behaviour presented a stark contrast to the random directional changes of growing hyphae observed on agar, which resulted in the curled morphology and overall a thorough exploration of the agar substrate in the three spatial dimensions. Generally, this behaviour expressed by the *N. crassa ro-1* mutant, triggered by the confinement, was more pronounced than the change in growth dynamics of the wild type. Therefore, it appeared that the *ro-1* mutant responded more severely to confinement than the wild type.

Growth dynamics in 100 μm channels

The 100 μm channels confined the fungi more significantly and caused an equally intense response by both *Neurospora crassa* strains as those observed in the 1000 μm wide channels. The *N. crassa* wild type navigated the channels in a manner that was much more biologically efficient than the mutant, because it branched significantly less, thus allocating less biomass per invaded area. Fig 3C represents a set of four successive diamond structures inside a 100 μm wide channel. In all cases, the hyphae grew into a fixed direction and in three out of four cases, the 100 μm connection channels between the individual structures were navigated without forming lateral branches. The growth dynamics of the *ro-1* mutant was similar to that observed in the larger channels. Hyphae initially tended to gradually align or attach to the closest wall available and then followed it over long distances. Subsequently, the branching increased significantly towards the respective confining wall the hyphae had aligned or attached to. In conjunction

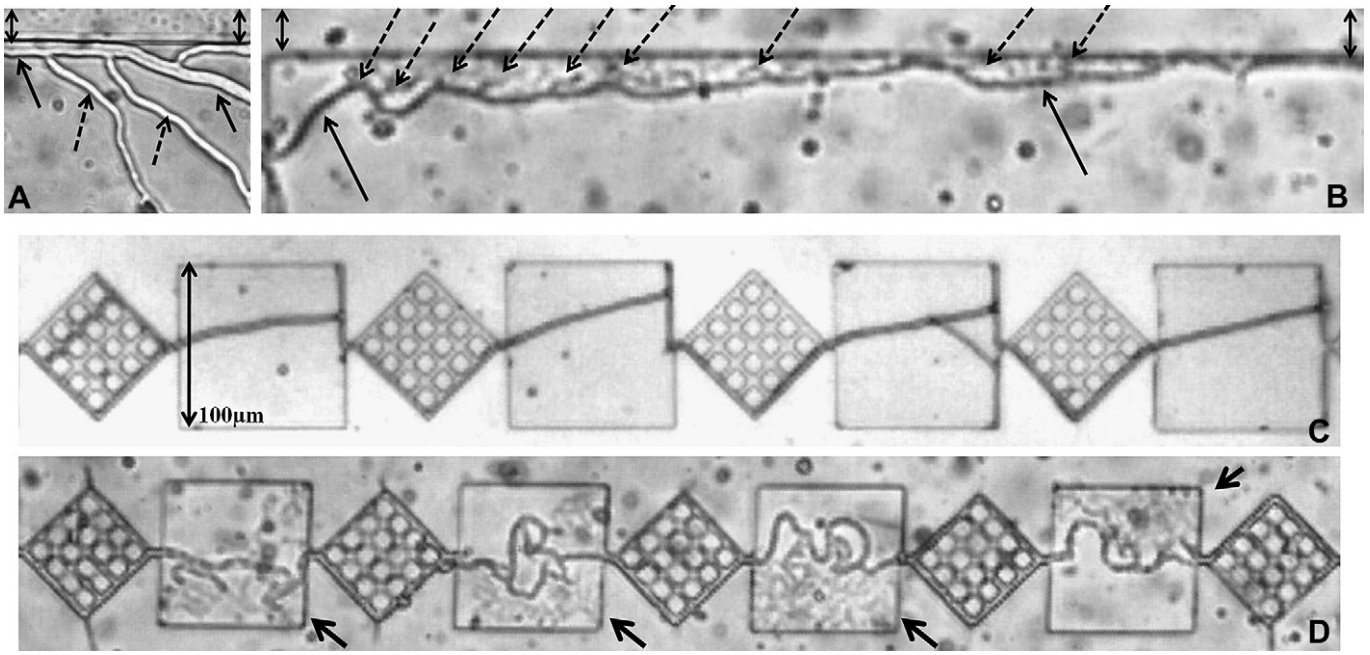

Fig 3 – Overview over the morphologies and growth dynamics of the *N. crassa* wild type and *ro*-1 type strain in the 1000 μm (A) – wild type, (B) – *ro*-1 mutant and 100 μm (C) – wild type, (D) – *ro*-1 mutant wide channels. The double arrows in (A) and (B) indicate the PDMS wall in the image. The solid arrows indicate the parent hypha whereas the dashed arrows indicate daughter hyphae that in (A) have branched away from the confining wall and in (B) have branched towards the confining wall thereby pushing the parent hypha away from the wall. The black arrows in (D) indicate the handedness of the branching of the *ro*-1 mutant in the 100 μm wide channel. Initially, the parent hyphae grew closer to the confining walls, started branching towards the walls and were ultimately pushed away by the bulk of the branches (see also Movie 3, Supplementary Data).

with the increased branching, the parent hyphae were pushed away from the wall they initially aligned to into the channel. Fig 3D represents a set of five successive diamond structures navigated by the mutant strain (Movie 3 in the Supplementary Data). The snapshot represents the end of the process, where the parent hypha had been pushed into the middle of the channel by a large number of daughter hyphae that occupied a significant portion of the 100 μm wide channels.

Supplementary videos related to this article can be found at doi:10.1016/j.funbio.2011.02.003.

Growth dynamics in microfluidic channel structures

In contrast to the previous channels, the microfluidic structures provided a tight confinement in the three spatial dimensions. Both *Neurospora crassa* strains navigated the two microfluidic test structures successfully, i.e., one or more hyphae reached the exit, and in similar times of approximately 4.5 h for the small maze structure. Compared with the significantly divergent values of the growth parameters, i.e., branching angle, branching distance, and the apical extension velocity for the two strains as measured on agar, the values reached similar values for both strains in the respective confined environments. The response of both strains did not require a temporal or spatial adjustment period, but occurred rather instantaneously upon entering the microfluidic structures. This lead us to the conclusion that the fungus relied on both wall contact-based and wall contact-independent space-searching mechanisms (Movies 1–4, Supplementary Data, for movies of the wild type and the *ro-1* mutant in the small maze and diamond structures respectively). In particular, in the case of the *N. crassa* wild type, the exhibited growth behaviour comprised a complementary combination of structure-dependent measurable parameters and structure-independent, general growth patterns.

Measurable growth parameters

The measurable growth parameters of both strains in the various environments tested are summarised in Table 1. The exit *versus* entrance rates for both strains in both structures were established by rating the total number of hyphae exiting the structures *versus* the total number of hyphae that entered the structures initially. For the small maze, the exit *versus* entrance rates were 0.90 for the wild type and 0.73 for the *ro-1* mutant. In the diamond structure, an increased number of hyphae, formed by branching and exiting the structure was responsible for exit *versus* entrance rates larger than one (1.23 for the wild type, 1.35 for the *ro-1* mutant).

The three measured growth parameters, i.e., apical extension velocity, branching angle, and branching distance, appeared to be strongly dependent on the specific layout of the test structures used. The growth parameter that was most affected by microconfinement was the apical extension velocity. Comparing the velocities of both strains on agar, that of the *ro-1* mutant was approximately two-thirds of that of the wild type. Within the microfluidics structures, the mutant extended at slightly faster rates in both test structures (Table 1). However, the trend in the data was similar for both species. In contrast, the trends for the branching angle and the branching distance were significantly different. Thus, it appears that the mutation had the least impact on the apical extension velocity. The branching angle and branching distance parameters underwent a larger change for the wild type compared with the *ro-1* mutant. As the design of the structures imposed changes of directions at approximately 90° angles, the branching angle for the wild type increased two-fold during microconfinement (Fig 4A and C). However, because of the periodicity of the obstacles in the diamond structure, the branching angle for the wild type had a significantly smaller standard deviation than for the complex small maze structure, thus demonstrating the precise adaptability of the fungus to the invaded microenvironment. In contrast, the *ro-1* mutant maintained similar values of the branching angle of around 90° on agar, in the small maze (Fig 4C) and in the diamond structure (Fig 4D). The average branching distance of the wild type on agar exceeded the edge length of the structures by a factor of two. Inside the microfluidic test structures, this value decreased to 43.1 μm in the diamond and 23.5 μm in the small maze structure, respectively, which represents a nine-fold decrease. This increased branching resulted in significant hyphal ramification, which was specific for individual structure designs. Branches were typically directed towards channel openings and branching towards solid walls or obstacles appeared suppressed. In contrast, the branching distance of the *ro-1* mutant varied within a few tens of micrometres on agar and in microconfinement. Branching was not exclusively directed towards channel openings and branching suppression during wall contact was not as evident as for the wild type thus providing further evidence that the mutation had the largest impact on the branching.

The observed similarity of the measurable growth parameters of both strains inside the microfluidic test structures was unexpected.

General growth patterns

The observation of both strains within the microfluidic test structures showed that neither formed conidia throughout the duration of the experiment. The absence of conidia inside the microfluidic structures could have stemmed from the inability of the fungi to form aerial hyphae, which are a prerequisite for the formation of spores. Furthermore, hyphal fusion events were absent even though hyphae frequently encountered each other. These encounters were principally resolved by the hyphae continuing growth in the determined directions, crossing over, and superposing each other (Fig 4C and D). Once a channel crossing was filled with hyphae, any approaching hypha ceased growth upon encountering the blocked partition. Due to the confinement in the microfluidics channels, the growing hyphae experienced frequent wall collisions, to which both examined *Neurospora crassa* strains exhibited a number of different behavioural traits as discussed below. These behavioural patterns have not previously been observed on agar and therefore it is reasonable to hypothesise that they are triggered by the microconfinement. Most of these responses were independent of the design of the microfluidic channel layouts, in contrast to the measurable growth parameters that varied considerably for the respective structures.

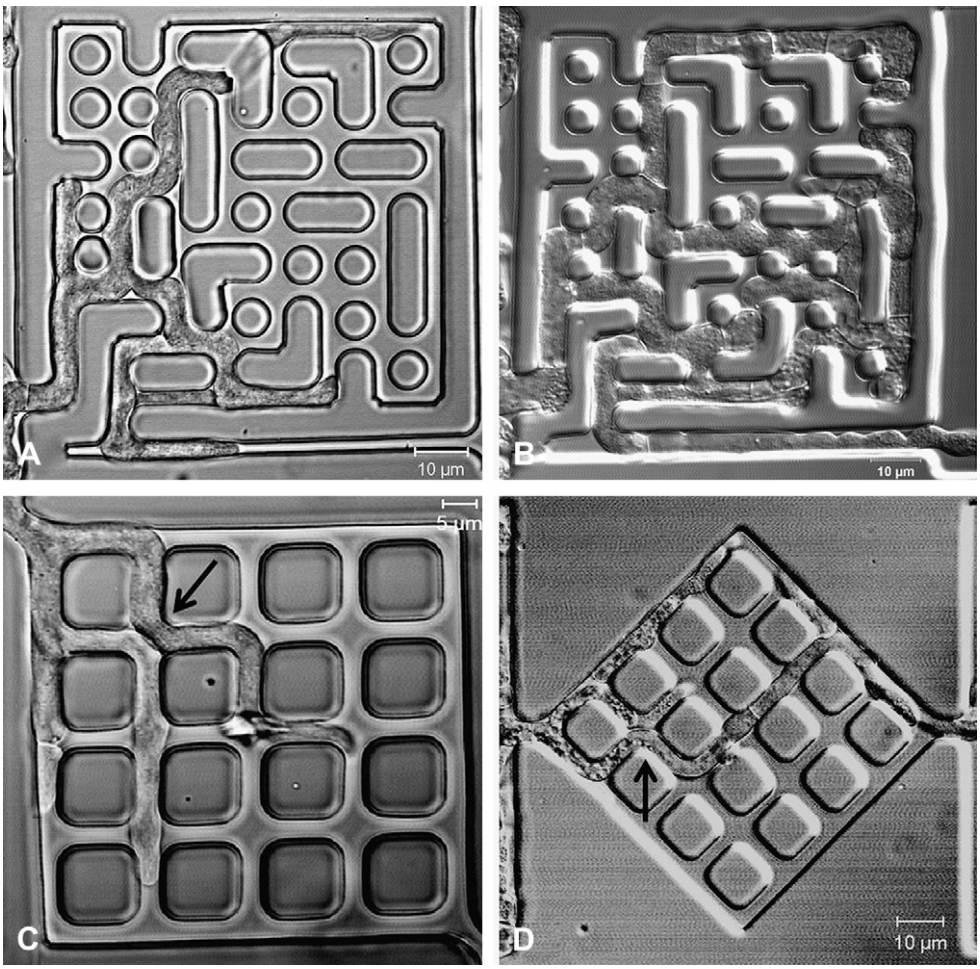

Fig 4 – Comparison of the *N. crassa* strains in the tested microfluidic structures: (A) – wild type in small maze, (B) – *ro-1* in small maze, (C) – wild type in diamond, (D) – *ro-1* in diamond. The structures were entered by the strains from the left. The black arrows in (C) and (D) indicate channel sections where two hyphae share the available space by superposing each other without fusing. Please also see Movies 1–4 in the Supplementary Data for movies of each species solving a small maze and a diamond structure.

Biomass distribution in the microfluidic channel structures. Biomass distributions were determined as the occupancy of the channels by *Neurospora crassa* hyphae averaged over a number of different experiments *i*, e.g., 80 experiments for the wild type in the small maze. A graphical representation of these normalised distributions, showing a colour coded density map according to the calculated scale factors sf_i is depicted in Fig 5. The normalised biomass distributions of the two *N. crassa* strains for the diamond structure were very similar, with the majority of hyphae concentrating on the outer paths surrounding the pattern of 16 pillars. In the small maze, the biomass distributions seemed to differ to a larger extent. The *ro-1* mutant appeared to invest more biomass on filling the volume of the maze, whereas for the wild type, the biomass appeared to be concentrated along the shortest path through the maze.

Additional to the biomass distribution in the structures, we used the scale factor as a measure to quantify the average occupancy of the structures. The average scale factors $\overline{sf}$ of the *N. crassa ro-1* mutant in the microfluidic test structures were 10 % larger than those of the wild type, i.e., it invested more biomass in the navigation process. The fact that the growing hyphae are supported with nutrients transported from the colony centre, located on the agar plug adjacent to the microfluidic channels, makes the formation of biomass energetically more expensive. Considering this, the result suggests that the *ro-1* mutant invests more resources in navigating the structures and is therefore less biologically efficient in navigating the artificial microconfinement.

Directional memory. One of the two most prominent growth patterns exhibited by the wild type is 'directional memory' (Hanson *et al*. 2006) which is the return of hyphae to their initial growth directions after temporary diversion by a physical obstacle. On agar, the hyphae extended by following fixed polarisation axes determined at the respective branching points. The maintenance of these polarisation axes appeared to be the basis of the directional memory observed in microconfinement. After a collision with an obstacle, the hyphae of the wild type adapted their extension closely to the obstacle

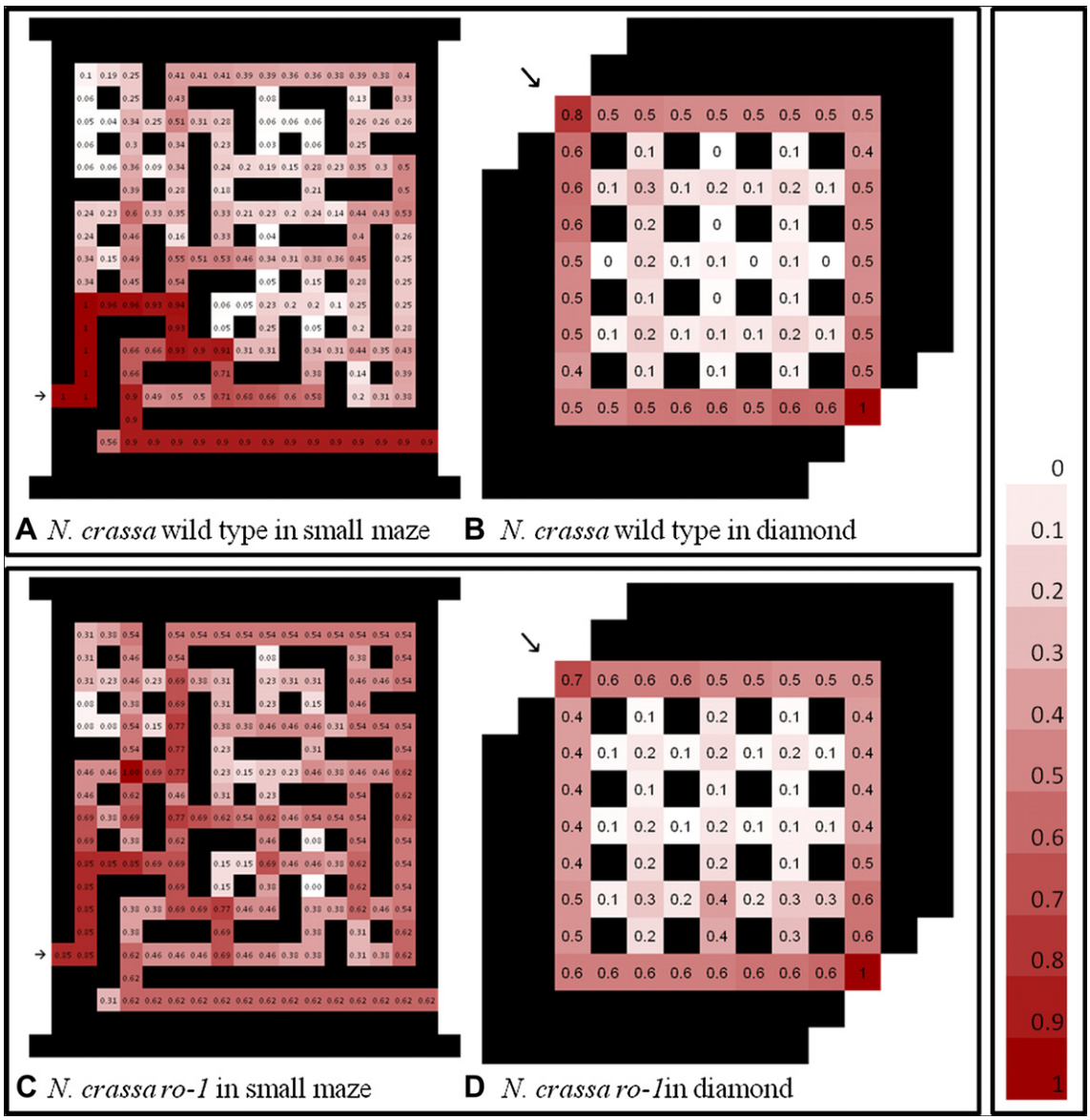

Fig 5 – Overview over the biomass distributions of the *N. crassa* wild type and the *ro-1* mutant inside the small maze and the diamond structure. The distributions were determined as the occupancy of the channels with *N. crassa* hyphae averaged over a number of different experiments, (A): $n = 80$; (B): $n = 185$; (C): $n = 20$, (D): $n = 11$. The distributions were normalised to the area with the highest density of hyphae.

in the direction closest to that of their directional memory until they could re-establish the original trajectory, usually maintaining close wall contact. The hyphal polarisation axis usually returned to the initial direction within a maximum deflection of $\pm 20^{\circ}$. It appeared that the directional memory established at the branching point did not decay with increasing hyphal length or the duration of exposure to the microconfined geometry (Fig 6A and Fig 3C). Directional memory was a dominant characteristic of the wild type growth, but not always beneficial for navigation through the microfluidic structures. In particular for the small maze, which required a 180° turn by the hypha, directional memory would lead the initial parent hypha into a dead end (Movie 1, Supplementary Data), only following the solution path for a limited distance. However, apical splitting induced by the geometry (see below) resulted in a continued extension along the shortest path and therefore in a high biomass density along the shortest solution path through the maze (Fig 5A).

The *Neurospora crassa ro-1* mutant did not exhibit directional memory. As this strain lacked the maintenance of a fixed hyphal growth direction on agar, this observation confirms the hypothesis that the directional memory is based on the initial establishment of a polarisation axis for fungal hyphae. However, the mutant strain also progressed through the confinement away from the colony centre.

Hit and split. The second of the most prominent observed growth characteristics was collision-induced apical splitting

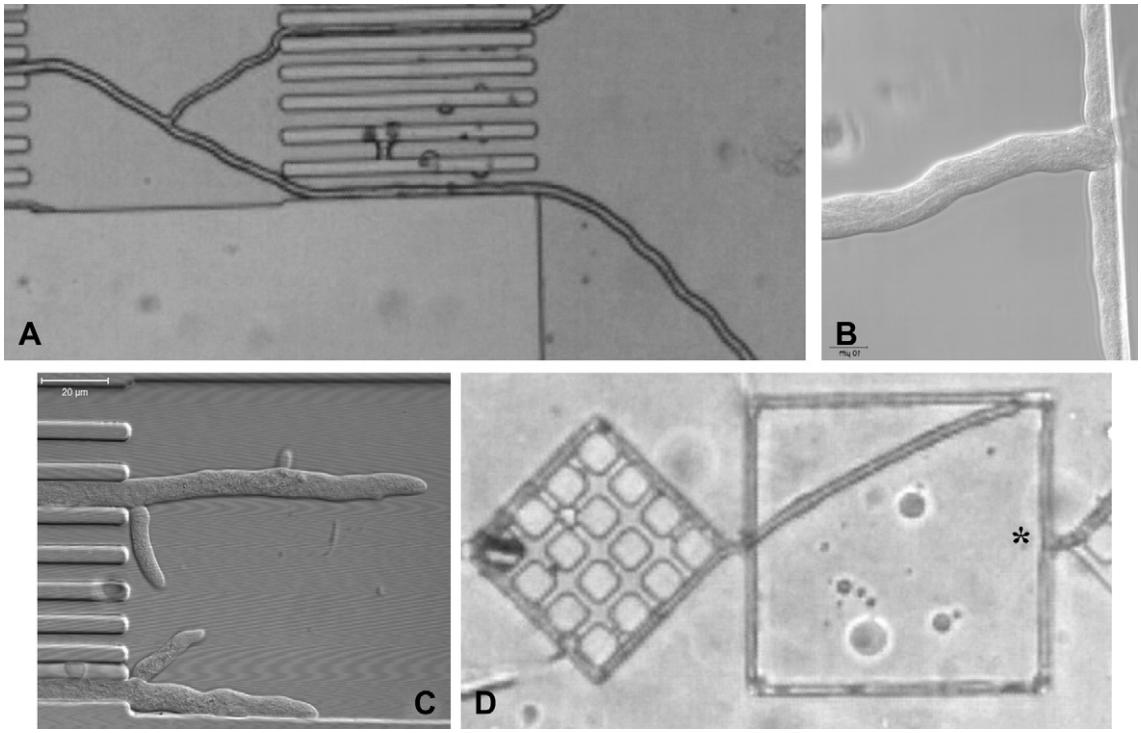

Fig 6 – General growth parameters: all images show the *N. crassa* wild type and all hyphae initially entered the field of view from the left. (A) Directional memory, (B) hit and split – apical split after a head-on collision with an obstacle, (C) increased branching after bottlenecks, (D) nestling and corner turns. (C) Comprises a set of parallel channels with varying widths. The widths range from 2 μm at the bottom to 10 μm at the top with an increment of 1 μm. In figure (D), the hypha initially entered the 100 μm wide intermediate channel exiting the previous diamond structure in the middle of the left-hand wall. Following its polarisation axis, it hit the top right corner, turning it successfully. The asterisk in (D) indicates a branch that emanated from a parent hypha directly into a channel opening while the hypha followed the wall geometry towards the bottom right corner where it turns. Growth was continued along the bottom wall, followed by two more corner turns, eventually leading back to the initial collision point in the top right corner.

of the wild type hyphae (Fig 6B). When a hypha collided with an obstacle at a steep angle (>55°), it normally bulged uniformly and then split into two daughter branches that grew simultaneously around the obstacle in opposite directions from the collision point. Usually, the daughter branches emanated from the branching point with a similar velocity independent of the collision angle of the parent hypha with the obstacle.

Handedness. The wild type branched preferentially into channel openings and away from an obstacle while branching was suppressed at the hypha-PDMS interface during close contact with the geometry. This indicates that the wild type used an efficient sensing mechanism to identify the channel openings in order to trigger a branch (asterisk in Fig 6D). Thus, we suggest that branching and the direction of the branches were determined by the geometry, ultimately resulting in the structure-dependent branching angles and distances.

The handedness of the branching pattern in *N. crassa ro-1* that was observed in the 1000 μm and 100 μm wide channels appeared to be significantly reduced in the microfluidic test structures (Movies 3 and 4, Supplementary Data) and resulted in a branching pattern that was less suppressed by direct wall contact, as compared with the wild type. It appeared that branches were formed rather randomly with a rate similar to the one on agar medium and thus it appears that the sensing mechanism determining channel openings in the wild type was affected by the mutation.

Increased branching after bottlenecks. Close confinement within channels of smaller width than the average hyphal diameter, triggered branching in the wild type upon exiting the confinement. Fig 6C represents an image of two hyphae grown through a 2 μm and 8 μm wide channel respectively. These channels had a length of 100 μm and in this case, both were narrower than the initial hyphal diameter prior to penetration. At the end of both channels, the hyphae branched immediately upon exiting suggesting that these branches were triggered by the geometry of these locations. One possible explanation could be that although a branching trigger was building up while the hypha was within the confinement, the close wall contact suppressed it thus 'overwriting' any trigger for branching. Once the geometrical confinement had ended, the signal ceased and a branch was formed. This observed behaviour could rest on the same response mechanism as the directed branching into channel openings exhibited by the wild type. Importantly, the *ro-1* mutant did not show increased branching after bottlenecks.

Nestling. Growing the *Neurospora crassa* wild type on raised surface patterns demonstrated that the strain exhibited a particular affinity for sharp edges (Held *et al.* 2009c). In the microfluidic structures, this behaviour seemed to translate into a close contact between the hypha and the constraining geometry, in case the initial growth direction was obstructed (Fig 6A and D). Hyphae did not deflect from the walls or 'nose' along the walls (like the hyphae of *Pycnoporus cinnabarinus* (Hanson *et al.* 2006)) but adapted their polarisation axes to one parallel to the confining wall (when the collision angle was smaller than 55°, otherwise an apical split was triggered). This indicated a very flexible hyphal apex capable of 'moulding' to the micron-sized geometrical features. During the growth following the geometry, the hyphal apex was distorted from a parabolic shape and was skewed towards the confining wall (Fig 6C). However, once the initial growth direction became available again, the hyphae readily detached from the geometry, resuming their respective directional memories.

As has been demonstrated in the 1000 μm and the 100 μm wide channels, the *ro-1* mutant expressed a tendency to attach to the closest vertical confining walls of the PDMS channels and to follow them for long periods. This behaviour was distinctly different compared to that of the wild type. The wild type only attached to the wall once the initial growth direction was obstructed by the geometry. The *ro-1* mutant, which lacks directional memory, attached to the geometry regardless. When a hypha entered the small maze structure, it usually attached to the right-hand side of the channel and followed it closely. Thus, it was partly guided along the shortest path through the maze. This growth pattern resulted in an overall biomass distribution (Fig 5C) with a high density of biomass along a path close to the solution path – overlaid by increased branching.

Corner turns. Both *Neurospora crassa* strains were very effective in turning corners. Fig 6D represents a hypha of the wild type following the geometry over directional changes of more than 360°. The hypha grew along the four outer walls of the intermediate 100 μm wide channel. It did not turn in the position marked by the asterisk but a branch was triggered that continued growth through the row of diamond structures. The hyphal response to a corner collision was similar to the one observed during head-on collisions with obstacles. The hyphal apex bulged uniformly upon collision, but as there was only one available growth direction that was not obstructed by the geometry or the hypha itself, it could only expand into this direction. Eventually, a branch was formed continuing growth into this direction indicating a change in the polarisation axis of the hypha. For the *ro-1* mutant, the hyphal response was not as evident and often involved frequent branching. The hyphal apex would bulge as observed for the wild type, but it appeared that the determination of a new polarisation axis was less directed occasionally resulting in the formation of several branches at the collision point with a variety of polarisation axes.

Table 2 summarises the general growth patterns of both strains: exposed to the same microfluidic structures, the wild type and the *ro-1* mutant responded fundamentally different. Considering the similarity of the measurable growth parameters (Table 1), this difference is indeed remarkable.

Table 2 – Summary of the general growth patterns of the *N. crassa* wild type and the *ro-1* mutant observed on agar and within microfluidic test structures.

Feature	*N. crassa* wild type	*N. crassa* *ro-1*
On agar		
Drawn to agar surface	Yes	No
Formation of aerial hyphae followed by sporulation	Yes	Yes Conidia form in dense clumps
In microfluidics		
Directional memory	Yes	No
Collision-induced apical splitting (Hit and Split)	Yes	No
Increased branching after bottlenecks	Yes	No
Nestling	Yes	No
Handedness	No	Yes
Branching away from confinement	Yes (additionally branching into channel openings)	No

Biological implications of the observed behaviour

Both *Neurospora crassa* strains were able to solve artificial microfluidic networks. The response of the *N. crassa* wild type to three-dimensionally enclosed channels surpassed the response observed on open, patterned surfaces (Held *et al.* 2009c). Combining the findings in this study with previous results for another species (Hanson *et al.* 2006), we suggest that filamentous fungi generally respond actively and rapidly to geometrical confinements on the microscale, hence making fungal thigmotropism an important parameter that should be considered in the study of their growth dynamics.

Considering the particular flexibility of the apex of the *N. crassa* wild type and its adaptability to the geometrical features, we infer that these characteristics could be biologically beneficial in its natural environment, which consists of burned plant matter after fires. This material is usually very brittle and vulnerable to natural influences like wind and rain. The ability of *N. crassa* to attach closely to the material might result in an overall stabilisation of the natural nutrient source, which is beneficial for the formation and support of fruit bodies.

The behaviour of both *N. crassa* strains appeared to vary significantly with the channel width, i.e., the narrower the channels, the more significant the response and the alteration in measurable growth parameters. These response mechanisms seemed to fall into two categories: wall contact-based and wall contact-independent sensing mechanisms. Both strains navigated the microfluidics structures with similar measurable growth parameters and found the respective exits; however, the two strains applied fundamentally independent sets of structure-independent growth patterns. The mutation of the *ro-1* strain resulted in branching angles and branching distances on agar that resembled those parameters in the microfluidic structures, i.e., navigating the structure did not require a significant adaptation of these parameters. There are two possible implications from these observed growth dynamics: (i) the space-searching algorithms of *N. crassa* are very robust

and changes to them by this particular mutation appear to be negligible; or (ii) the mutant strain accidentally exhibited optimal growth patterns to solve these types of structures and might not be able to navigate different geometries. The growth dynamics in the 1000 μm and 100 μm wide channels could be an indication for the latter case, but are not conclusive.

Conclusions

We presented a methodology for the study of the dynamic behaviour of filamentous fungi based on the use of purposefully designed microfluidic test structures and the potential value of this methodology for obtaining insight into the biological basics of fungal growth. The application of PDMS-based channels and channel networks with dimensions similar to the size of the fungal cell diameter instead of homogeneous media resulted in geometry-specific and geometry-independent thigmotropic responses of the hyphal growth behaviour, thus revealing distinct, so far unreported space-searching strategies. The observed behaviour was strongly dependent on the degree as well as the complexity of confinement. It appeared that the possible sensing mechanisms did not exclusively rely on wall contact and resulted in an instantaneous growth response.

Acknowledgements

This study was funded by a Leverhulme Trust grant. The *N. crassa* wild type strain was provided by the Liverpool School of Biological Sciences Culture Collection. We thank Prof. Abe P. Lee and Dr. Lisen Wang of the University of California, Irvine, for the fabrication of the silicon masters.

REFERENCES

Apoga D, Barnard J, Craighead HG, Hoch HC, 2004. Quantification of substratum contact required for initiation of *Colletotrichum graminicola* appressoria. *Fungal Genetics and Biology* **41**: 1–12.

Bartnicki-Garcia S, Hergert F, Gierz G, 1989. Computer simulation of fungal morphogenesis and the mathematical basis for hyphal (tip) growth. *Protoplasma* **153**: 46–57.

Beadle GW, Tatum EL, 1945. *Neurospora*. II. Methods of producing and detecting mutations concerned with nutritional requirements. *American Journal of Botany* **32**: 678–686.

Bechinger C, Giebel K-F, Schnell M, Leiderer P, Deising HB, Bastmeyer M, 1999. Optical measurements of invasive forces exerted by appressoria of a plant pathogenic fungus. *Science* **285**: 1896–1899.

Binz M, Lee AP, Edwards C, Nicolau DV, 2010. Motility of bacteria in microfluidic structures. *Microelectronic Engineering* **87**: 810–813.

Boddy L, 1999. Saprotrophic cord-forming fungi: meeting the challenge of heterogeneous environments. *Mycologia* **91**: 13–32.

Boddy L, Hynes J, Bebber DP, Fricker MD, 2009. Saprotrophic cord systems: dispersal mechanisms in space and time. *Mycoscience* **50**: 9–19.

Boswell G, Jacobs H, Ritz K, Gadd G, Davidson F, 2007. The development of fungal networks in complex environments. *Bulletin of Mathematical Biology* **69**: 605–634.

Brand A, Vacharaksa A, Bendel C, Norton J, Haynes P, Henry-Stanley M, Wells C, Ross K, Gow NAR, Gale CA, 2008. An internal polarity landmark is important for externally induced hyphal behaviors in *Candida albicans*. *Eukaryotic Cell* **7**: 712–720.

Brunswick H, 1924. *Untersuchungen über die Geschlechts- und Kernverhältnisse bei der Hymenomycetengattung Coprinus, Jena*.

Chen CS, Mrksich M, Huang S, Whitesides GM, Ingber DE, 1998. Micropatterned surfaces for control of cell shape, position, and function. *Biotechnology Progress* **14**: 256–363.

Darrah PR, Tlalka M, Ashford A, Watkinson SC, Fricker MD, 2006. The vacuole system is a significant intracellular pathway for longitudinal solute transport in basidiomycete fungi. *Eucaryotic Cell* **5**: 1111–1125.

Desai TA, 2000. Micro- and nanoscale structures for tissue engineering constructs. *Medical Engineering and Physics* **22**: 595–606.

Duffy DC, McDonald JC, Schueller OJA, Whitesides GM, 1998. Rapid prototyping of microfluidic systems in poly(dimethylsiloxane). *Analytical Chemistry* **70**: 4974–4984.

Emerson S, 1963. Slime, a plasmoid variant of *Neurospora crassa*. *Genetica* **34**: 162–182.

Evans CS, Hedger JN, 2001. Degradation of plant cell wall polymers. In: Gadd GM (ed), *Fungi in Bioremediation*. Cambridge University Press, Cambridge, United Kingdom, pp. 1–26.

Folch A, Toner M, 1998. Cellular micropatterns on biocompatible materials. *Biotechnology Progress* **14**: 388–392.

Freitag M, Hickey PC, Raju NB, Selker EU, Read ND, 2004. GFP as a tool to analyze the organization, dynamics and function of nuclei and microtubules in *Neurospora crassa*. *Fungal Genetics and Biology* **41**: 897–910.

Fricker MD, Lee JA, Bebber DP, Tlalka M, Hynes J, Darrah PR, Watkinson SC, Boddy L, 2008. Imaging complex nutrient dynamics in mycelial networks. *Journal of Microscopy* **231**: 317–331.

Garnjobst L, Tatum EL, 1967. A survey of new morphological mutants in *Neurospora crassa*. *Genetics* **57**: 579–604.

Ghantasala MK, Harvey EC, Sood DK, 1999. *Excimer Laser Micromachining of Structures Using SU-8, Micromachining and Microfabrication Process Technology V*, 1st edn. SPIE, Santa Clara, CA, USA, pp. 85–91.

Ghantasala MK, Hayes JP, Harvey EC, Sood DK, 2001. Patterning, electroplating and removal of SU-8 moulds by excimer laser micromachining. *Journal of Micromechanics and Microengineering* **11**: 133–139.

Girbardt M, 1969. Die Ultrastruktur der Apikalregion von Pilzhyphen. *Protoplasma* **67**: 413–441.

Gougouli M, Koutsoumanis KP, 2010. Modelling growth of *Penicillium expansum* and *Aspergillus niger* at constant and fluctuating temperature conditions. *International Journal of Food Microbiology* **140**: 254–262.

Griscom L, Degenaar P, Denoual M, Morin F, 2002. Culturing of neurons in microfluidic arrays. *Microtechnologies in Medicine and Biology 2nd Annual International IEEE-EMB Special Topic Conference on*, 160–163

Grove SN, Bracker CE, 1970. Protoplasmic organization of hyphal tips among fungi: vesicles and Spitzenkörper. *Journal of Bacteriology* **104**: 989–1009.

Hanson KL, Nicolau DVJ, Filipponi L, Wang L, Lee AP, Nicolau DV, 2006. Fungi use effective algorithms for the exploration of microfluidic networks. *Small* **2**: 1212–1220.

Harris SD, Momany M, 2004. Polarity in filamentous fungi: moving beyond the yeast paradigm. *Fungal Genetics and Biology* **41**: 391–400.

Held M, Binz M, Edwards C, Nicolau DV, 2009a. In: Farkas DL, Nicolau DV, Leif RC (eds), *Dynamic Behaviour of Fungi in Microfluidics: a Comparative Study*, 1st edn SPIE, San Jose, CA, USA, pp. 718213–718219.

Held M, Edwards C, Nicolau D, 2009b. Fungal intelligence; or on the behaviour of microorganisms in confined micro-environments. *Journal of Physics: Conference Series* **178**.

Held M, Edwards C, Nicolau DV, 2008. In: Farkas DL, Nicolau DV, Leif RC (eds), *Examining the Behaviour of Fungal Cells in Microconfined Mazelike Structures*, 1st edn SPIE, San Jose, CA, USA, pp. 68590–68599.

Held M, Komaromy A, Fulga F, Edwards C, Boysen RI, Hearn MTW, Nicolau DV, 2009c. Dynamic behaviour of microorganisms on microstructures. *Microelectronic Engineering* **86**: 1455–1458.

Held M, Lee AP, Edwards C, Nicolau DV, 2010. Microfluidics structures for probing the dynamic behaviour of filamentous fungi. *Microelectronic Engineering* **87**: 786–789.

Hoch HC, Staples RC, Whitehead B, Comeau J, Wolf ED, 1987. Signaling for growth orientation and cell differentiation by surface topography in *Uromyces*. *Science* **235**: 1659–1662.

Jiang X, Bruzewicz DA, Wong AP, Piel M, Whitesides GM, 2005. Directing cell migration with asymmetric micropatterns. *Proceedings of the National Academy of Sciences USA* **102**: 975–978.

Kane RS, Takayama S, Ostuni E, Ingber DE, Whitesides GM, 1999. Patterning proteins and cells using soft lithography. *Biomaterials* **20**: 2363–2376.

Kasuga T, Glass NL, 2008. Dissecting colony development of *Neurospora crassa* using mRNA profiling and comparative genomics approaches. *Eukaryotic Cell* **7**: 1549–1564.

Katz D, Goldstein D, Rosenberger RF, 1972. Model for branch initiation in *Aspergillus nidulans* based on measurements of growth parameters. *Journal of Bacteriology* **109**: 1097–1100.

Klumpp S, Lipowsky R, 2003. Traffic of molecular motors through tube-like compartments. *Journal of Statistical Physics* **113**: 233–268.

Kumamoto CA, 2008. Molecular mechanisms of mechanosensing and their roles in fungal contact sensing. *Nature Reviews Microbiology* **6**: 667–673.

Leclerc E, Sakai Y, Fujii T, 2003. Cell culture in 3-dimensional microfluidic structure of PDMS(polydimethylsiloxane). *Biomedical Microdevices* **5**: 109–114.

Lee JN, Park C, Whitesides GM, 2003. Solvent compatibility of poly(dimethylsiloxane)-based microfluidic devices. *Analytical Chemistry* **75**: 6544–6554.

Lötters JC, Olthuis W, Veltink PH, Bergveld P, 1997. The mechanical properties of the rubber elastic polymer polydimethylsiloxane for sensor applications. *Journal of Micromechanics and Microengineering: Structures, Devices, and Systems* **7**: 145–147.

McDonald JC, Duffy DC, Anderson JR, Chiu DT, Wu H, Schueller OJA, Whitesides GM, 2000. Fabrication of microfluidic systems in poly(dimethylsiloxane). *Electrophoresis* **21**: 27–40.

Menz W, Mohr J, Paul O, 2001. *Microsystem Technology*. WILEY-VCH Verlag GmbH, Weinheim, Germany.

Merkel TC, Bondar VI, Nagai K, Freeman BD, Pinnau I, 2000. Gas sorption, diffusion, and permeation in poly(dimethylsiloxane). *Journal of Polymer Science Part B: Polymer Physics* **38**: 415–434.

Molin P, Gervais P, Lemiere JP, Davet T, 1992. Direction of hyphal growth: a relevant parameter in the development of filamentous fungi. *Research in Microbiology* **143**: 777–784.

Momany M, 2002. Polarity in filamentous fungi: establishment, maintenance and new axes. *Current Opinion in Microbiology* **5**: 580–585.

Momany M, Richardson EA, Sickle CV, Jedd G, 2002. Mapping woronin body position in *Aspergillus nidulans*. *Mycologia* **94**: 260–266.

Nicolau DV, Nicolau JDV, Solana G, Hanson KL, Filipponi L, Wang L, Lee AP, 2006. Molecular motors-based micro- and nano-biocomputation devices. *Microelectronic Engineering* **83**: 1582–1588.

Park S, Wolanin PM, Yuzbashyan EA, Lin H, Darnton NC, Stock JB, Silberzan P, Austin R, 2003a. Influence of topology on bacterial social interaction. *Proceedings of the National Academy of Sciences USA* **100**: 13910–13915.

Park S, Wolanin PM, Yuzbashyan EA, Silberzan P, Stock JB, Austin RH, 2003b. Motion to form a quorum. *Science* **301**: 188.

Park TH, Shuler ML, 2003. Review – integration of cell culture and microfabrication technology. *Biotechnology Progress* **19**: 243–253.

Riquelme M, Bartnicki-Garcia S, 2004. Key differences between lateral and apical branching in hyphae of *Neurospora crassa*. *Fungal Genetics and Biology* **41**: 842–851.

Riquelme M, Reynaga-Pena CG, Gierz G, Bartnicki-Garcia S, 1998. What determines growth direction in fungal hyphae? *Fungal Genetics and Biology* **24**: 101–109.

Riquelme M, Roberson RW, McDaniel DP, Bartnicki-Garcia S, 2002. The effects of ropy-1 mutation on cytoplasmic organization and intracellular motility in mature hyphae of *Neurospora crassa*. *Fungal Genetics and Biology* **37**: 171–179.

Robinson PM, Bolton SK, 1984. Autotropism in hyphae of *Saprolegnia ferax*. *Transactions of the British Mycological Society* **83**: 257–263.

Ryan FJ, Beadle GW, Tatum EL, 1943. The tube method of measuring the growth rate of *Neurospora*. *American Journal of Botany* **30**: 784–799.

Seiler S, Plamann M, 2003. The genetic basis of cellular morphogenesis in the filamentous fungus *Neurospora crassa*. *Molecular Biology of the Cell* **14**: 4352–4364.

Sia SK, Whitesides GM, 2003. Microfluidic devices fabricated in poly(dimethylsiloxane) for biological studies. *Electrophoresis* **24**: 3563–3576.

Silverman-Gavrila LB, Lew RR, 2003. Calcium gradient dependence of *Neurospora crassa* hyphal growth. *Microbiology* **149**: 2475–2485.

Singhvi R, Kumar A, Lopez GP, Stephanopoulos GN, Wang DIC, Whitesides GM, Ingber DE, 1994a. Engineering cell shape and function. *Science* **264**: 696–698.

Singhvi R, Stephanopoulos G, Wang DIC, 1994b. Effects of substratum morphology on cell physiology. *Biotechnology and Bioengineering* **43**: 764–771.

Sugden KEP, Evans MR, Poon WCK, Read ND, 2007. Model of hyphal tip growth involving microtubule-based transport. *Physical Review E (Statistical, Nonlinear, and Soft Matter Physics)* **75** (art. No. 031909).

Trinci APJ, 1974. A study of the kinetics of hyphal extension and branch initiation of fungal mycelia. *Journal of General Microbiology* **81**: 225–236.

Trinci APJ, Collinge AJ, 1973. Structure and plugging of septa of wild type and spreading colonial mutants of *Neurospora crassa*. *Archives of Microbiology* **91**: 355–364.

Uchida M, Mouriño-Pérez RR, Freitag M, Bartnicki-García S, Roberson RW, 2008. Microtubule dynamics and the role of molecular motors in *Neurospora crassa*. *Fungal Genetics and Biology* **45**: 683–692.

van Delft F, van de Laar R, Verschuuren M, Platzgummer E, Loeschner H, 2010. Charged particle nanopatterning (CHARPAN) of 2D and 3D masters for flexible replication in substrate conformal imprint lithography (SCIL). *Microelectronic Engineering* **87**: 1062–1065.

Vaughn LE, Davis RH, 1981. Purification of vacuoles from *Neurospora crassa*. *Molecular and Cellular Biology* **1**: 797–806.

Verdín J, Bartnicki-Garcia S, Riquelme M, 2009. Functional stratification of the Spitzenkörper of *Neurospora crassa*. *Molecular Microbiology* **74**: 1044–1053.

Watters MK, Humphries C, De Vries I, Griffiths AJF, 2000a. A homeostatic set point for branching in *Neurospora crassa*. *Mycological Research* **104**: 557–563.

Watters MK, Virag A, Haynes J, Griffiths AJF, 2000b. Branch initiation in *Neurospora* is influenced by events at the previous branch. *Mycological Research* **104**: 805–809.

Wright GD, Arlt J, Poon WCK, Read ND, 2007. Optical tweezer micromanipulation of filamentous fungi. *Fungal Genetics and Biology* **44**: 1–13.

Ziauddin J, Sabatini DM, 2001. Microarrays of cells expressing defined cDNAs. *Nature* **411**: 107–110.